

Preliminary study of the mechanical characteristics implementation of friction stir welded AA2024 joints by adding pure copper

Sara Bocchi^{1, a*}, Gianluca D'Urso^{1, b} and Claudio Giardini^{1, c}

¹ University of Bergamo - Department of Management, Information and Production Engineering, Via Pasubio 7b, 24044, Dalmine (BG), Italy

^asara.bocchi@unibg.it, ^bgianluca.d-urso@unibg.it, ^cclaudio.giardini@unibg.it

Keywords: Friction Stir Welding, Aluminium, Solid State Diffusivity

Abstract. In the present paper, the mechanical properties of a AA2024 welded by Friction Stir Welding (FSW) were examined, both homogeneously and using a commercial pure copper sheet positioned between the edges to be welded in two configurations, T and C. The temperature trends reached during the FSW process were extrapolated through the development of a simulative model, to select the best combination of parameters to use in the experimental phase of the campaign. After that, the FSWed homogeneous and heterogeneous joints were executed and analysed. From the mechanical point of view, Rockwell B hardness tests and tensile tests were performed. It was possible to evidence a good relationship between the hardness distribution and the presence of the copper, especially at the nugget. On the contrary, the tensile tests executed orthogonally to the welding direction, showed a reduction of the tensile strength and of the real elongation percentage in the aluminium-copper heterogeneous FSWed joints.

Introduction

The Friction Stir Welding (FSW) is one of the most significant technological developments in metal joining of the last thirty years and it is considered a sustainable technology thanks to its energy efficiency. Friction Stir Welding is a welding technology developed by The Welding Institute (TWI) [1]. This solid-state mechanical joining technique is used to make joints between similar or dissimilar materials that are difficult to weld with conventional fusion techniques, such as sintered materials, magnesium, copper, Inconel, titanium, metal matrix composites and thermoplastics [2]. It is also used for high-strength aluminium alloys, which are difficult to join using traditional techniques due to their typical microstructural alteration during ageing hardening. In fact, the precipitates that are created thanks to the thermal treatment, interact with the dislocations within the matrix, influencing their mobility, and, consequently, the mechanical behaviour of the material. The morphology of the precipitates, the orientation, the distance between them and the degree of their coherence with the matrix contribute to the effectiveness of the precipitates themselves as a barrier to the movement of dislocations [3]. In particular, the interactions between dislocations and precipitates determine the mechanical behaviour of aluminium-copper alloys and, for the Al-Cu-(Mg) system, the precipitation sequence is as follows [4]:

Solid supersaturated solution (SSSS) \rightarrow GP Zone \rightarrow θ'' \rightarrow θ' \rightarrow θ (Al₂Cu).

The precipitates represent a common microstructural feature of high strength aluminium-copper alloys, they are formed on the faces of the face-centred cubic structure of the matrix, and they provide an anisotropic contribution to the performance of the material stresses. At temperatures immediately below the solubilization, the Guinier-Preston (GP) zones begin to nuclear very rapidly at an increasing rate as the elapsed time decreases. These zones grow in such a way as to minimise the rate of increase in the deformation energy of the precipitates and the matrix.

The second intermediate phase, called θ'' , is still coherent with the matrix, resides on its planes and has a tetragonal structure. This phase is wider than the GP zones and maintains the same chemical composition.

As the ageing process continues, a final metastable precipitate (θ') arises, with a tetragonal structure composed of Al_2Cu . These precipitates are semi-coherent to the aluminium matrix and swell with increasing ageing due to the surface reduction force.

The final equilibrium precipitate (θ) is mainly inconsistent with the matrix and can be nucleated directly from the supersaturated solution if the ageing temperature is high enough (about 300°C), or even at lower temperatures if the kinetic and thermodynamic conditions in the material are favourable. However, it was found that the phase diagram cannot explicitly explain what happens during the FSW process because it is constructed when the phases are in equilibrium. Knowing that the FSW process involves significant thermal changes, it is safe to assume that there is not enough time to have an equilibrium chemical reaction. The nucleation of the first metastable phases, which have a lower thermodynamic driving force, but a lower nucleation barrier due to greater coherence with the matrix, is therefore kinetically favourable [5].

One of the advantages of dissimilar soldering of copper to aluminium is that it can reduce the formation and growth of the layer formed by intermetallic compounds, introducing strong plastic deformation, and thus increasing the mechanical properties of the joint. The main advantages of diffusion are the obtainment of high-quality bonds and the possibility of producing joints with low porosity and good continuity along the weld [6].

Through a specific study on the solid-state diffusion of copper in aluminium, W. Bedjaoui et al. has shown that commercial 2xxx series aluminium and pure copper can be successfully joined using a solid-state diffusion welding process [7]. Furthermore, the increase in temperature and time during the diffusion bond leads to the formation of different types of intermetallic compounds, the dimensions of which vary as the parameters used vary.

The goal of this research is to improve the mechanical properties of a welding joint, operated by Friction Stir Welding between two AA2024 aluminium sheets, using a copper sheet positioned between the edges to be welded. By exploiting the solid-state diffusivity of copper in aluminium, the arrangement of copper within the aluminium alloy, through the passage of copper precipitates into the alloy which improve its mechanical characteristics, was ensured. The pair of parameters, rotational speed and advancing feed of the tool, which allows it to stay within the area of the aluminium-copper diagram in which the hardening precipitates are formed θ' , is identified through finite element simulations. After that, an experimental campaign was conducted and subsequent mechanical tests, Rockwell hardness and tensile tests, were executed.

Materials and Methods

A 3D FEM Lagrangian model was set up using the commercial software DEFORM 3D™. The tool was modelled as a rigid object using AISI-1045 steel as reference material (defined between 20°C and 1100°C). The plates to be welded were modelled as a single plastic workpiece made of Aluminium-2024 (defined between 300°C and 500°C). Both steel and aluminium with their material flow stress data were chosen among those available in the Deform library database.

The assumption to consider the tool as a rigid object and the workpiece as plastic is reasonable because of the significantly higher yield strength of the steel tool with respect to the yield strength of the aluminium workpiece. Finally, the workpiece was discretized using 80000 tetrahedral elements, as shown in Fig. 1. Regarding the thermal part of the simulation, the considered parameters are reported in Tab. 1, as they were optimised in a previous work [8].

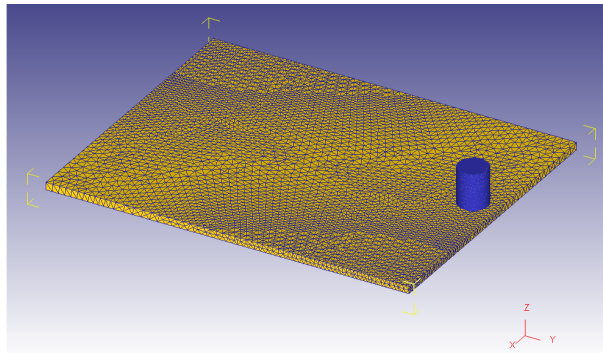


Fig. 1: Mesh of the aluminium workpiece.

Table 1: Thermal and friction parameters considered for the simulations.

Parameter	Value
Heat exchange with the environment	0.02 N/(mm·s·°C)
Friction coefficient aluminium-tool	1
Thermal conductivity	450 N/(mm·s·°C)
Aluminium emissivity	0.7
Heat transfer coefficient aluminium-tool	10000 N/(mm·s·°C)

As regards the process parameters, it was identified from a literature review a range of acceptable values to be considered for FSW welding of an AA2024 joint [9]–[13]. The chosen parameters are reported in Tab. 2.

Table 2: Process parameters used for the simulations.

Rotational speed (rpm)	Advancing feed (mm/min)
600-800-1000	40-120-200

Each combination of parameters was simulated. At the end of each simulation, the temperature trends at the nugget (0 and 5 mm from the centre of the weld), the TMAZ and the HAZ (20 mm and 35 mm from the welding line respectively) were evaluated.

The sheets were experimentally welded using the best combination of parameters resulting from the simulations performed: in order to obtain the right interaction between copper and aluminium.

The experimental campaign was performed using a CNC machine. Butt joints were carried out on AA2024-T3 sheets having a thickness equal to 4 mm (chemical composition and mechanical properties declared by the supplier in Tab. 3 and Tab. 4).

Table 3: AA2024-T3 composition.

Al	Si	Fe	Cu	Mn	Mg	Zn	Ti	Cr
bulk	0.06	$\frac{0.0}{9}$	4.50	0.46	1.40	0.08	0.04	0.03

Table 4: AA2024-T3 mechanical properties.

Yield Strength (YS) [MPa]	Ultimate Tensile Strength (UTS) [MPa]	Max strain [%]
344	464	16

A simple tool with a frustum of cone pin shape (pin minimum and maximum diameters equal to 4 and 6 mm, pin height equal to 3.9 mm) and flat shoulder (diameter equal to 16 mm) was considered. For all the welding, the tool inclination at 3° and the tool penetration depth into the sheets at 3.99 mm were fixed.

A homogeneous welding was carried out between two sheets of AA2024-T3 and then two welds were performed in which a commercially pure copper sheet (thickness equal to 0.1 mm) was interposed between the aluminium edges: one in a T- and one in a double C-configuration, as shown in Fig. 2. The thin copper sheet was ultrasonically cleaned in an acetone bath and then manually bent into the desired shape.

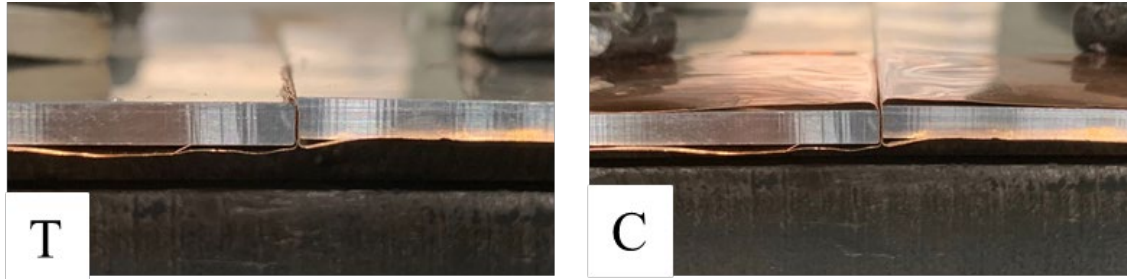


Fig. 2: T and double C copper configurations.

Rockwell B hardness tests (HRB) were performed following a 5 mm spaced grid in the central zone of the top of the specimen to avoid border effects, according to ISO 6508. Three profiles of indentations were carried out moving from the joint axis to the base material until the hardness of the base material was reached.

Tensile tests were executed orthogonally to the welding direction on the specimens having the welding nugget placed in the middle of gage length, according to UNI EN ISO 6892-1:2019. For the tests, a testing machine Galdabini with a load cell of 50 kN was used. The tests were carried out under speed control (1.2 mm/min). For the calculation of the engineering strain ϵ , strain gauges were applied to each sample.

Results and Discussion

From the simulations conducted in Deform, the temperature trends obtained in the four characteristic zones described in the methodology section were extrapolated: the peak temperatures reached were considered, to choose the best conditions to ensure the diffusivity of the copper within the aluminium (Tab. 5).

At the end of the experimental campaign, it was possible to note the absence of macroscopic defects in the homogeneous welding of AA2024, and in both welds made with copper interposed between the aluminium sheets (Fig. 3).

Table 5: Maximum temperatures obtained with the simulations. The pair of parameters chosen to conduct the experimental campaign is highlighted in orange.

Parameters		Temperatures [°C]			
[rpm]	[mm/min]	Centre [0 mm]	Nugget [5 mm]	TMAZ [20 mm]	HAZ [35 mm]
600	40	482.53	410.94	404.20	399.52
600	120	421.91	329.40	253.14	241.32
600	200	370.69	263.19	171.39	156.85
800	40	521.32	465.21	457.46	452.04
800	120	467.03	349.85	270.46	258.00
800	200	392.74	287.70	190.59	168.25
1000	40	485.46	409.89	403.48	398.69
1000	120	520.44	426.27	326.44	312.03
1000	200	463.77	360.46	219.94	199.23

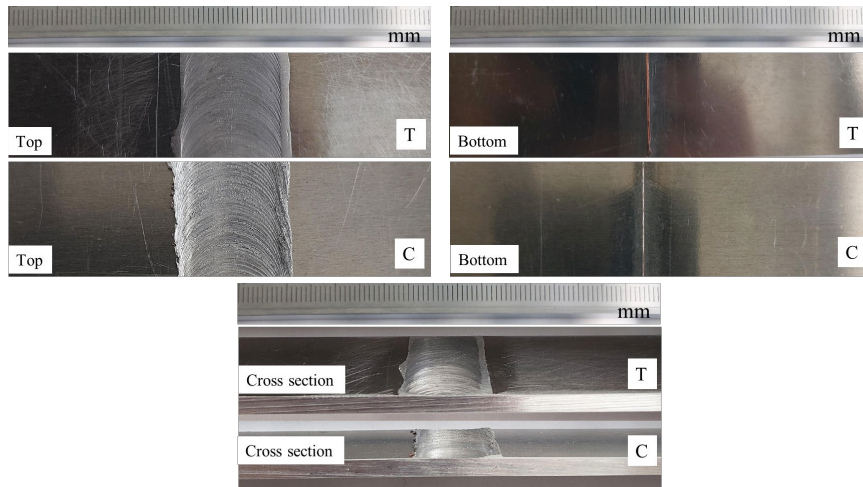


Fig. 3: Tops, bottoms, and cross sections of the heterogeneous joints AA2024-Cu.

Fig. 4 shows the graphs of the Rockwell B hardness tests performed both on the homogeneous welding AA2024-AA2024 and on the welds obtained with the addition of copper.

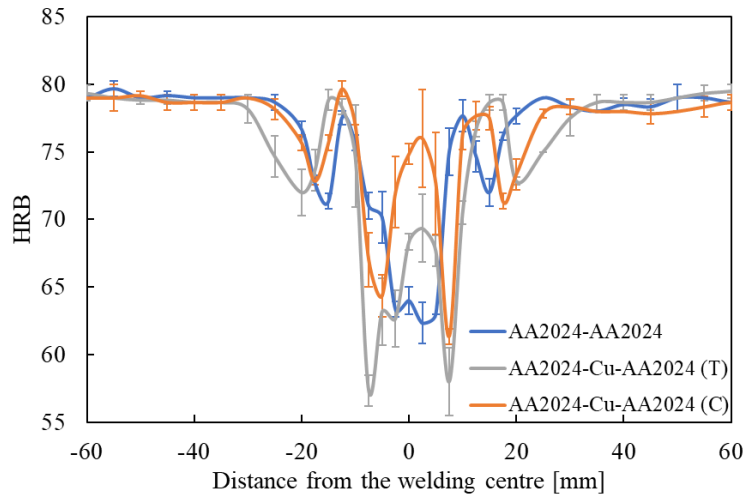


Fig. 4: HRB of the homogeneous and heterogeneous Friction Stir Welded joints.

With respect to homogeneous welding, the addition of copper has led to changes in the trend of the hardness curves. It can be observed that the minimum points of hardness have lower values in both the heterogeneous joints than in homogeneous welding, especially in the T-configuration. This behaviour could be attributable to the formation of embrittlement precipitates linked to the thermo-mechanical history of the area involved, that it is exactly on the nugget boundaries. The lowest hardness point in the homogeneous alloy is at the nugget, whilst in both heterogeneous configurations, these lower peaks are translated towards the base metal by about 5 mm to the right and about 5 mm to the left of the weld line.

Furthermore, on average there is an increase in hardness in the central area between -2.5 mm and +5 mm from the centre of the weld of about 4 HRB for the T-configuration and 11 HRB for the C-configuration. The increase in hardness of the C-configuration compared to the T-configuration is probably due to the greater quantity of copper used during processing, which is therefore able to form part of the brittle precipitates as well as the hardening precipitates. From the comparison it is also possible to observe a shift towards the base material of the minimum hardness points of the HAZ, of 5 mm for the T configuration and of 2.5 mm for the C configuration, with a less marked increase in hardness.

The addition of copper has determined an increase in hardness in the central area of the nugget, this is due to the passage in solid solution of the copper in the aluminium matrix, causing the formation of hardening precipitates, and the displacement of the minimum hardness values in the HAZ area and in the area between the nugget and the TMAZ towards the base metal causing a widening of the curves with their consequent removal from the nugget.

From the graph proposed in Fig. 5, it is possible to see the trend of the stress as the deformation varies tested and the fracture points for each condition.

In general, the addition of copper resulted in a reduction in the tensile strength (UTS). The UTS was 350.5 MPa for homogeneous welding, while for the C- and T-configurations it was, respectively, 301.75 MPa and 285.75 MPa. Furthermore, thanks to the tensile tests it was possible to ascertain that the addition of copper also led to a reduction in the percentage elongation at break. This value was equal to 2.56% for homogeneous welding, while for the C- and T- configurations it was 1.27% and 1.21%, respectively. It is also evident that, for all conditions, the fracture occurred preferentially in the central area of the nugget.

The reduction in the UTS and the percentage elongation at break compared to homogeneous welding is probably due to the presence of small layers of hard and brittle intermetallic precipitates (IMC) that are formed during welding, and which cause a reduction in mechanical strength. The formation of these very brittle intermetallic precipitates in a dissimilar AA2024-copper was demonstrated also by R. Khajeh et al. [14]. From the graph it is also possible to note that in the C-configuration the UTS and the percentage elongation are greater than those of the T-configuration. This is probably due to the higher amount of copper conveyed during welding in the C-configuration with respect to the T one. In fact, as the quantity of copper increases, the presence of the same in the weld increases, therefore in addition to the formation of the hard and brittle intermetallic precipitates, there is a greater formation of hardening precipitates by diffusion in the solid state which counteract the reduction of mechanical resistance due to IMC.

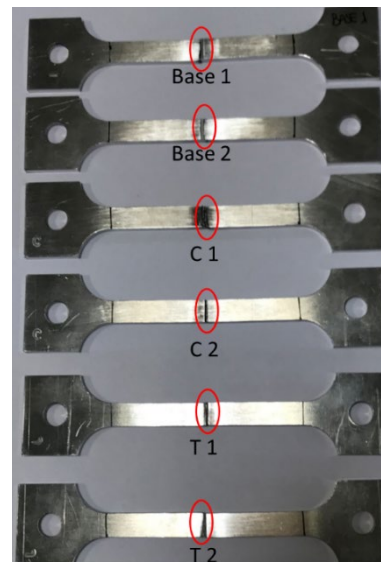
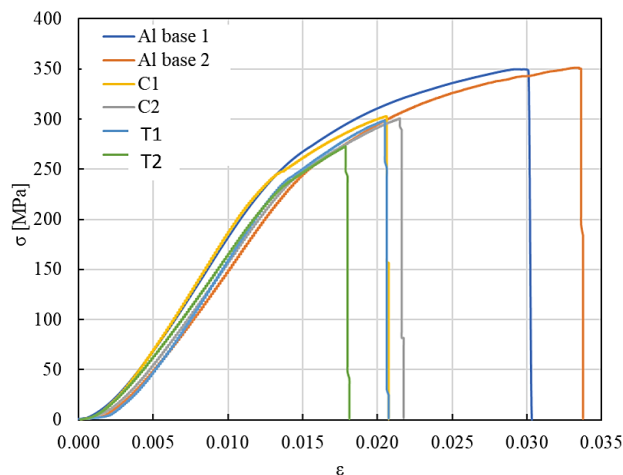


Fig. 5: On the left: tensile tests of the homogeneous and heterogeneous Friction Stir Welded joints (the number 1 and the number 2 are referred to the number of repetitions). On the right: fracture points of the homogeneous and heterogeneous joints.

Conclusions

The mechanical properties of the AA2024 welded by Friction Stir Welding were examined, both homogeneously and using a copper sheet positioned between the edges to be welded in two configurations, T and C.

Through an initial simulation phase and a subsequent experimental phase, it was possible to observe that:

- The parameters chosen from the simulations ($S=800$ rpm and $f=40$ mm/min) proved to be suitable for all the welds, as they were free of defects and with good surface finishes.
- Rockwell hardness tests demonstrated that the addition of copper caused changes in hardness in the various characteristic areas of the joint. In particular, it increased the hardness in the central area of the nugget by 4 Rockwell points in the T configuration and 11 Rockwell points in the C configuration. Furthermore, it determined the shift of the hardness minima towards the base material.
- From the tensile tests it was found that the addition of copper resulted in a reduction in the tensile strength and the percentage elongation at break compared to homogeneous welding. However, the C-configuration has been observed to exhibit a higher tensile strength and percentage elongation at break than the T-configuration.

In conclusion, it can be stated that the improvement of the mechanical characteristics of a FSWed AA2024 by adding commercially pure copper to the interface of the aluminium edges to be welded, has been achieved partially but it is a good strategy that deserves to be studied.

Having observed that the mechanical characteristics of the C-configuration were superior to those of the T-configuration, to obtain better results it is suggested to orient the next studies in identifying copper configurations that allow the use of a greater quantity of copper in the welding. Moreover, new combinations of parameters had to be studied since it is not certain that the parameters optimised for the AA2024 alone are also optimal parameters for heterogeneous welds with copper, even if they do not show macroscopic defects.

References

- [1] W. M. Thomas, E. D. Nicholas, J. C. Needham, M. G. Murch, P. Templesmith, and C. J. Dawes, "GB Patent application no. 9125978.8," 1991.
- [2] M. Tabasi, M. Farahani, M. K. B. Givi, M. Farzami, and A. Moharami, "Dissimilar friction stir welding of 7075 aluminum alloy to AZ31 magnesium alloy using SiC nanoparticles," *Int. J. Adv. Manuf. Technol.*, vol. 86, no. 1–4, pp. 705–715, Sep. 2016. <https://doi.org/10.1007/s00170-015-8211-y>
- [3] H. Sehitoglu, T. Foglesong, and H. J. Maier, "Precipitate effects on the mechanical behavior of aluminum copper alloys: Part I. Experiments," *Metall. Mater. Trans. A*, vol. 36, no. 3, pp. 749–761, Mar. 2005. <https://doi.org/10.1007/s11661-005-0190-4>
- [4] C. Sigli, F. De Geuser, A. Deschamps, J. Lépinoux, and M. Perez, "Recent advances in the metallurgy of aluminum alloys. Part II: Age hardening," *Comptes Rendus Physique*, vol. 19, no. 8. No longer published by Elsevier, pp. 688–709, 01-Dec-2018. <https://doi.org/10.1016/j.crhy.2018.10.012>
- [5] M. Jariyaboon et al., "The effect of welding parameters on the corrosion behaviour of friction stir welded AA2024–T351," *Corros. Sci.*, vol. 49, no. 2, pp. 877–909, Feb. 2007. <https://doi.org/10.1016/j.corsci.2006.05.038>
- [6] E. B. Hannech, N. Lamoudi, N. Benslim, and B. Makhloufi, "Intermetallic formation in the aluminum-copper system," *Surf. Rev. Lett.*, vol. 10, no. 4, pp. 677–683, Apr. 2003. <https://doi.org/10.1142/S0218625X03005396>
- [7] W. Bedjaoui, Z. Boumerzoug, and F. Delaunois, "Solid-State Diffusion Welding of Commercial Aluminum Alloy with Pure Copper," *Int. J. Automot. Mech. Eng.*, vol. 19, no. 2, pp. 9734–9746, Jun. 2022. <https://doi.org/10.15282/ijame.19.2.2022.09.0751>

- [8] M. Quarto, S. Bocchi, G. D', N. A. Urso, and C. Giardini, "Hybrid finite elements method-artificial neural network approach for hardness prediction of AA6082 friction stir welded joints," *Int. J. Mechatronics Manuf. Syst.*, vol. 15, no. 2/3, p. 149, 2022. <https://doi.org/10.1504/IJMMS.2022.124919>
- [9] T. Rajkumar, K. Raja, K. Lingadurai, S. D. Vetrivel, and A. Godwin Antony, "Interfacial microstructure analysis of AA2024 welded joints by friction stir welding," *J. New Mater. Electrochem. Syst.*, vol. 23, no. 2, pp. 123–132, Apr. 2020. <https://doi.org/10.14447/jnmes.v23i2.a09>
- [10] N. S. Abtan, A. H. Jassim, and M. S. Marmoos, "Study on the effects of rotational and transverse speed on temperature distribution through friction stir welding of AA2024-T3 aluminium alloy," *J. Adv. Res. Fluid Mech. Therm. Sci.*, vol. 53, no. 2, pp. 234–248, 2019.
- [11] M. Cabrini et al., "Stress corrosion cracking of friction stir-welded AA-2024 T3 alloy," *Materials (Basel)*, vol. 13, no. 11, Jun. 2020. <https://doi.org/10.3390/ma13112610>
- [12] A. W. El-Morsy, M. Ghanem, and H. Bahaitham, "Effect of Friction Stir Welding Parameters on the Microstructure and Mechanical Properties of AA2024-T4 Aluminum Alloy," *Eng. Technol. Appl. Sci. Res.*, vol. 8, no. 1, pp. 2493–2498, Feb. 2018. <https://doi.org/10.48084/etasr.1704>
- [13] S. Bocchi, M. Cabrini, G. D'Urso, C. Giardini, S. Lorenzi, and T. Pastore, "Stress enhanced intergranular corrosion of friction stir welded AA2024-T3," *Eng. Fail. Anal.*, vol. 111, Apr. 2020. <https://doi.org/10.1016/j.engfailanal.2020.104483>
- [14] R. Khajeh et al., "Microstructure, mechanical and electrical properties of dissimilar friction stir welded 2024 aluminum alloy and copper joints," *J. Mater. Res. Technol.*, vol. 14, pp. 1945–1957, Sep. 2021. <https://doi.org/10.1016/j.jmrt.2021.07.058>